Research Article

Hannah Kim, Yiwei Gao, Ethan Moran, Annyn Howle, Sean McSherry, Spencer Cira, and Andrej Lenert*

High Albedo Daytime Radiative Cooling for Enhanced Bifacial PV Performance

Abstract: We present a radiative cooling material capable of enhancing albedo while reducing surface temperature, specifically tailored for application as an artificial groundcover placed between rows of bifacial solar panels. Electrospinning a layer of polyacrylonitrile nanofibers, or nanoPAN, onto a polymer-coated silver mirror yields a total solar reflectance of 99 % (albedo of 0.96) and a thermal emittance of 0.80. The combination of high albedo and emittance is enabled by wavelength-selective scattering induced by the hierarchical morphology of nanoPAN, which includes both thin fibers and bead-like structures. During outdoor testing, the material outperforms the radiative cooling power of a state-of-the-art control by $\sim$20 W/m^2 and boosts the photocurrent produced by a commercial silicon cell by up to 6.4 mA/cm^2 compared to sand. These experiments validate essential characteristics of a high albedo groundcover with promising potential applications in thermal and light management of fielded bifacial panels.

Keywords: radiative cooling; ground albedo; bifacial; photovoltaics

1 Introduction

Regulating the temperature and diffuse light levels around fielded solar panels offers an opportunity to improve the performance and lifetime of existing and future photovoltaic (PV) installations. Solar heating significantly degrades both the efficiency (by $\sim$0.4 %°C^{-1}) and lifespan (by $\sim$7 %°C^{-1}) of solar panels [1]. Meanwhile, a large fraction of sunlight that is incident on the overall area of the solar installation remains unused. Even minor improvements in the performance of fielded panels can vastly impact the global energy system, given the expected multi-terawatt deployment of solar PV [2]. Tracking and bifacial PV technologies, which are being increasingly deployed in utility-scale solar installations, stand to particularly benefit from such thermal and light management.

Engineering the optical and thermal properties of the materials beneath and around the PV panels is gaining interest as a way to improve illumination and reduce panel temperatures. Research in agrivoltaics has shown that crops can reduce the local air temperature at the PV site, thereby reducing panel temperatures by up to 10 °C [3]. Meanwhile, simulations indicate that replacing natural groundcovers with artifical ground reflectors should substantially improve power output and energy yield of bifacial PVs [4–6]. Increasing ground albedo from 0.25 (typical for natural groundcover) to 0.50 can increase average bifacial electricity yields by 20% (global average) [4]. Reaching the highest bifacial gains requires optimizing the elevation and orientation of bifacial panels depending on latitude and albedo. Nonetheless, the promise of improved yields, easier cleaning (in a vertical orientation), and compatibility with leading PV technologies has driven growing interest in bifacial PV. That growth also motivates efforts to increase ground albedo and shape the landscape of the solar field [7].

Regarding thermal management, radiative cooling has emerged as a promising means of passively regulating temperature, with various applications ranging from energy savings in buildings [8] to atmospheric dew harvesting [9, 10] and enhancing personal thermal comfort [11, 12]. Daytime radiative cooling has been achieved by combining very high solar reflection (>90 %) with good thermal emission, specifically

Hannah Kim, University of Michigan, Ann Arbor, Ann Arbor, USA, hanmkim@umich.edu; 0000-0003-2885-4377
Yiwei Gao, University of Michigan, Ann Arbor, Ann Arbor, USA, yiweig@umich.edu; 0000-0002-8834-1664
Ethan Moran, University of Michigan, Ann Arbor, Ann Arbor, USA, ejmoran@umich.edu; 0009-0007-7672-9059
Annyn Howle, University of Michigan, Ann Arbor, Ann Arbor, USA, annyn@umich.edu; 0009-0008-3540-1548
Sean McSherry, University of Michigan, Ann Arbor, Ann Arbor, USA, mcsherry@umich.edu; 0000-0002-6855-0450
Spencer Cira, University of Michigan, Ann Arbor, Ann Arbor, USA, sgcira@umich.edu; 0009-0003-5343-7265
***Corresponding author: Andrej Lenert,** University of Michigan, Ann Arbor, Ann Arbor, USA, alenert@umich.edu; 0000-0002-1142-6627

within the atmospheric transparency windows (8 µm to 13 µm and 16 µm to 28 µm) [13, 14]. Given that peak solar irradiation ($\sim$1000 W/m^2) imparts about 10 times more heat than can be rejected by radiative cooling alone ($\sim$100 W/m^2), a 1 % increase in solar reflectance can lead to a 10 W/m^2 net gain in cooling power [15,16]. This insight has made suppressing solar heating a top priority, with various approaches such as multilayer emitters [17–20], particle-based coatings [21–27], and transparent insulating covers [28–34] used to achieve high solar-weighted reflectance (SR) [35,36]. Nonetheless, few approaches attain very high radiative cooling while providing the high albedo desired for redirecting sunlight toward bifacial panels. Furthermore, glare is an issue with many existing radiative coolers which can hinder the adoption of solar technologies [37–39].

Here, we fabricate and investigate materials with a combination of high albedo and excellent radiative cooling performance for potential use as an artificial groundcover in bifacial solar installations. Figure 1 shows representative images of the structure which was fabricated by coating a silicon wafer with a thin layer of silver as the back reflector (mirror), polydimethylsiloxane (PDMS) as the thermal emitter layer, and eletrospun polyacrylonitrile nanofibers (nanoPAN) as the high aldebo layer. Though other methods such as phase separation [32], phase-inversion [28,33], and sacrificial particle templating [31] can be used to fabricate porous polymer films, electrospinning provides excellent control over the morphology and polydispersity at length scales relevant to solar radiation [23, 29, 30]. The applied nanoPAN layer enhances reflectance in the ultraviolet (UV) and near infrared (IR) regions, resulting in a total solar-weighted reflectance of 99 $\pm$ 0.5%. Radiative cooling tests under clear sky conditions in Ann Arbor, MI, show temperature reduction and cooling power enhancements of $\sim$3 °C and $\sim$20 W/m^2, respectively, compared to the polymer-mirror control (without nanoPAN). The control is intentionally similar to an emitter that achieved state-of-the-art daytime radiative cooling performance under clear sky conditions in California [20], including cooling to 8 °C below ambient and a cooling power of $\sim$127 W/m^2 at ambient. Furthermore, replacing sand with the nanoPAN-based groundcover increases the photocurrent produced by a ground-facing latitude-tilted commercial silicon cell up to 6.42 mA/cm^2. This result corresponds to an estimated 18 % enhancement relative to the output of a typical silicon cell. Overall, the results shown here demonstrate the effectiveness of nanoPAN in enhancing radiative cooling and backside illumination. It is important to note that these functions of the material are demonstrated separately and at the scale of an individual cell in this proof-of-concept study. To evaluate the effects of the artificial groundcover on the working temperatures and energy yields of bifacial panels, future field testing in utility-scale installations is necessary. Specifically, additional field research is needed to assess the impact of ground-surface temperatures and albedo on the microclimate at the PV site and the panel temperatures. There is not enough information in literature to empirically estimate this effect, particularly across a broad range of climates and field types.

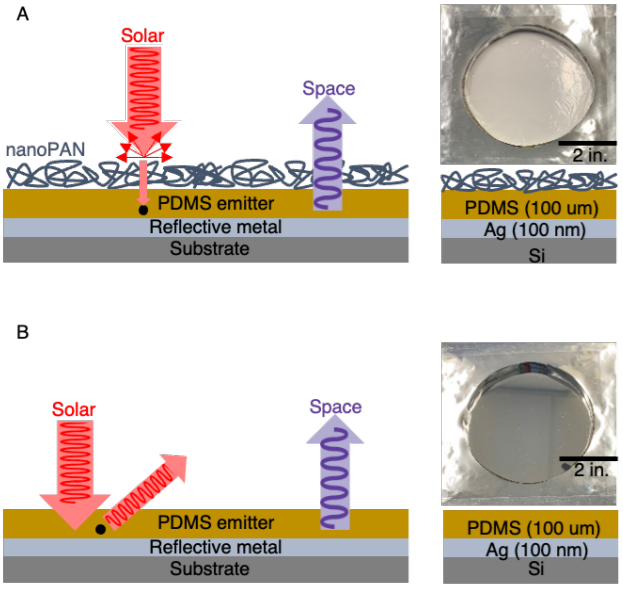

Fig. 1: (A) Radiative cooling artificial groundcover featuring a layer of electrospun beaded nanofibers (nanoPAN) and (B) polymer-mirror control representing a state-of-the-art specular radiative cooler.

2 Materials and Methods

2.1 Fabrication

The back reflector (10 nm Ti / 150 nm Ag) is deposited by electron beam deposition onto a 4 in Si wafer. The thermal emitter layer (1500 nm polydimethylsiloxane, *Dow Sylgard 184*) is added by spinning coating and cured for 15 minutes at 150 °C. The nanoPAN layer is deposited as previously [30] using a home-built electrospinning setup. The fiber morphology is optimized by controlling spinning parameters and the quantity

of PAN in solution. PAN powder (*Polysciences Inc.*) with an average MW of 200,000 is if fully dissolved in dimethylformamide (*Sigma*) at 6 wt% concentration by mixing overnight at 40 °C to 50 °C. The solution is loaded into a syringe with a 25-gauge blunt tip needle and placed in a syringe pump to ensure a constant flow rate. The PAN solution is electrospun at a flow rate of $0.4\,\mathrm{mL\,h^{-1}}$ and stage height of 11.5 cm for 80 min.

2.2 Radiative cooling measurements

Outdoor radiative cooling performance is evaluated as previously [30] using a custom rooftop test station in Ann Arbor (MI, USA). A transparent polyethylene convective cover is used to shield the samples from the wind. The variation of the global horizontal irradiance, on-site ambient temperature (measured using a shaded temperature logger adjacent to the samples, see [30] for details), and sample temperature is monitored throughout the tests. The reported cooling power of the nanoPAN sample is determined using outdoor measurements of its temperature with and without a constant heat input. The heated setup is identical to the stagnation temperature measurement except that a resistive heater is adhered to the sample with nanoPAN. Constant power is supplied to the heater and the resulting temperature of the sample is measured. This temperature along with the stagnation temperature is used to calculate the heat transfer coefficient (HTC) between the sample and the ambient, which is in turn used to find the cooling power at ambient temperature throughout the day. The assumption of a constant HTC is justified by the narrow temperature range (less than 10 °C). That HTC valueThe cooling power of the control is calculated using , along with its corresponding measured stagnation temperature. Differences in HTC are neglected because of the similarity in insulation and thermal emittances of the sample and control.

2.3 Backside illumination tests

Commercial silicon photovoltaic cells *(SunPower, Me1)* are mounted on a sand covered surface with an albedo value of approximately 30 %, which is close to the Earth's average albedo. The orientation of the photovoltaic cells is set to 42° tilt angle (local latitude of Ann Arbor, MI, USA). The distance between the bottom edge of the PV cell and the edge of the circular groundcover is 5 cm. The open-circuit voltage, V_{OC}, generated by the PV cells with and without a 10 cm-diameter circular nanoPAN groundcover is measured by a multimeter. The photovoltaic cells used in the tests are monofacial with the front surface (blue) facing true north (ground). The ground-facing monofacial cell mimics the backside of a bifacial solar cell and serves to determine a representative measure of the added photocurrent resulting from the higher ground albedo, which is the primary goal of this experiment. The measured voltage is averaged over three 20 min periods, corresponding to 3 hours before solar noon, solar noon, and 3 hours after solar noon.

Based on the experimentally measured V_{OC} values, the I_{L} is calculated using a single diode approximation given by:

$$I_{\mathrm{L}} = I_0(e^{\frac{qV_{\mathrm{OC}}}{nkT}} - 1) \tag{1}$$

where I_0 is the dark saturation current, n is the ideality factor, k is the Boltzmann constant, T is temperature of PV cell, and q is electron charge. I_0 and n are determined by fitting variable-illumination current-voltage curves using established procedures [40], which yields $n = 1.4$ and $I_0 = 1.118(10^{-7})$A.

3 Results and Discussions

3.1 Radiative properties of nanoPAN

The variation of the total reflectance versus wavelength for the nanoPAN groundcover (nanoPAN/PDMS/Ag) and mirrored control (PDMS/Ag) are shown in Figures 2A and 2B. The results for the control show lower reflectance starting around 0.5 µm and an overall SR of 97 %. The addition of the nanoPAN layer increases the total solar reflectance to 99 %. Substantial increases in reflectance are observed at wavelengths below 0.5 µm and between 1.4 µm to 2 µm. In contrast, the nanoPAN layer has a small effect on the long-wavelength properties relevant to thermal emission. The atmospheric weighted thermal emittance (ε) decreases only from 83 % to 80 % with the nanoPAN.

The key to achieving such selective enhancement in solar reflectance is the well-controlled hierarchical morphology of the nanofibers, which features cylindrical and ellipsoidal (bead-like) geometries. Figures 2C and 2D show images of the fabricated nanoPAN films and the bimodal size distribution associated with the fibers and beads obtained from >10 different SEM

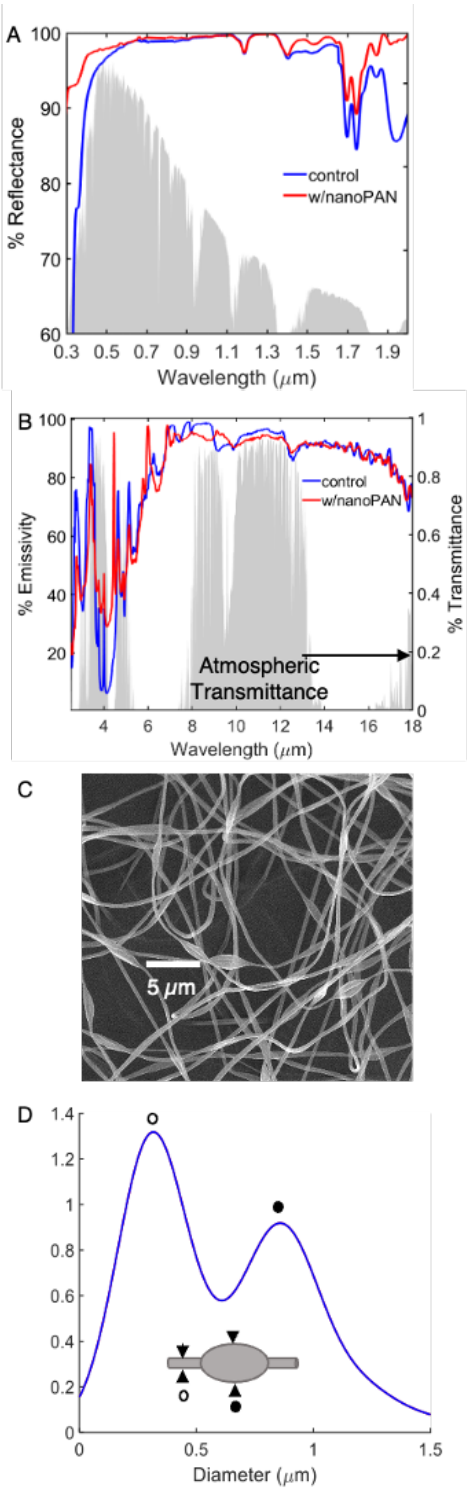

Fig. 2: (A) Measured total reflectance using UV-Vis with and without the nanoPAN layer. The AM1.5 G solar spectrum is shown for reference. (B) Measured total emissivity using FTIR. The atmospheric transmittance is shown for reference [41]. A 6 wt% PAN solution was used to fabricate beaded nanoPAN fibers via electrospinning after experimentally optimizing for high solar reflectance. (C) SEM image of 6 wt% electrospun nanoPAN fibers. (D) Hierarchical size distribution of the interconnecting fiber and beaded morphologies.

images using image processing software. Due to their characteristic length scales, the fibers are responsible for scattering shorter wavelengths and the beads for scattering longer solar wavelengths, as supported by simulations [29, 30].

Overall, the addition of nanoPAN increases the total SR by 2 % by addressing spectral ranges where the control is less reflective. Though this improvement may seem small, a 2 % improvement in SR (and negligible change in thermal emittance) is expected to yield a $\sim$20 W/m^2 gain in daytime cooling power. Furthermore, the nanoPAN layer increases the diffuse reflectance (or albedo) to approximately 95 % (SI Fig. S1), which is key to improving light collection in bifacial installations and gives the films a soft white appearance, minimizing unwanted glare. In addition, applying the nanoPAN layer to a PDMS-coated aluminum sheet increases solar reflectance from 76.7 % to 93.7 % (SI Fig. S2), demonstrating that the approach can be translated to lower cost substrates.

3.2 Radiative cooling performance

The radiative cooling performance of the nanoPAN sample (99 % SR) and its mirrored control (97 % SR) are assessed under clear sky conditions. Figure 3 shows the difference between the ambient temperature and the stagnation temperature ($\Delta T = T_{\text{amb}} - T_{\text{emit}}$), which is known as the temperature reduction or sub-ambient temperature. During the daytime, the temperature of the control hovers around ambient temperature while the nanoPAN sample is consistently below ambient. At night, both materials approach similar sub-ambient temperatures. The day to night difference in temperature reduction is approximately 9 °C for the control and 4 °C for the nanoPAN sample. These results show the that temperature of the nanoPAN groundcover is much less sensitive to variations in solar irradiance. Similar improvements relative to the control were observed on other test days with small differences due to variable weather conditions.

In addition to the stagnation temperature, the cooling power at ambient (Fig. 3D) is relevant to thermal management in solar fields. The average cooling power of the nanoPAN sample over the 14-hour period is $\sim$48.2 W/m^2. Imperfect sky conditions and parasitic heating of the enclosure are likely responsible for a lower cooling power than previously reported for emitters with comparable radiative properties, including the polymer-mirror emitter mentioned above [20].

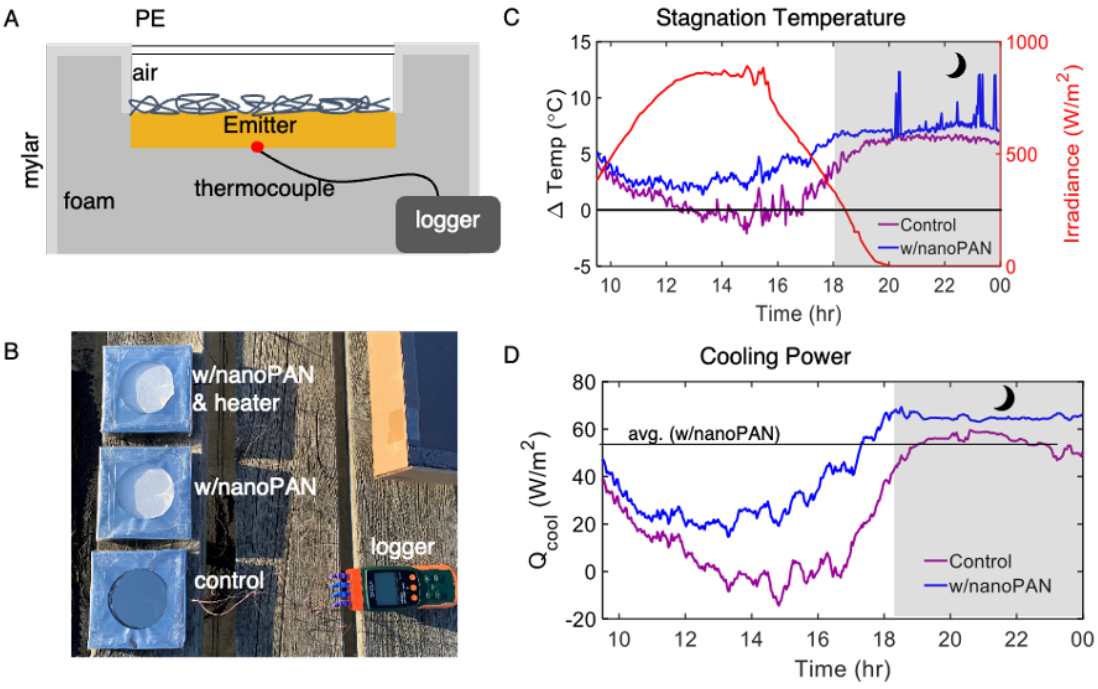

Fig. 3: Schematic (A) and images (B) of the outdoor setup used to evaluate radiative cooling performance. (C) Ambient temperature minus sample temperature (positive indicates better performance) comparing the nanoPAN sample to the control. (D) Corresponding cooling power at ambient temperature. (A 10-minute moving average is applied to decrease noise.)

Importantly, the afternoon cooling power increases by $\sim$20 W/m^2 due to the addition of the nanoPAN layer, consistent with the 2 % gain in absolute SR. One would expect that additional cooling power to translate to locations with utility-scale PV installations, most of which have better sky conditions than Ann Arbor, MI.

3.3 Backside illumination enhancement

In the backside PV illumination tests, we analyzed the the current and voltage gains mediated by the addition of the nanoPAN groundcover in a latitude-angle tilted north-south orientation, common in solar installations. Images and schematics describing the orientation and geometry of the field tests are shown in Fig. 4A. Sand is used as the baseline surface for these comparative tests because its albedo, shown in Fig. 4B, approximately matches the Earth's average. In contrast, the albedo of the nanoPAN groundcover is comparable to snow [42].

During the testing period, the nanoPAN-based surface consistently enhances the V_{OC} generated by the commercial PV cell compared to a sand surface. The enhancement reaches its highest value at solar noon. The voltage gain is attributed to additional light collected by the cell. Using the empirical cell model described above, we estimate absolute current gains ranging from 3.93 mA/cm^2 to 6.42 mA/cm^2 depending on the specific time of day, with the highest gain observed at solar noon. To put the current gains in context, a typical silicon solar cell produces around 35 mA/cm^2 to 40 mA/cm^2 under standard test conditions. Thus, the nanoPAN cover can add a substantial amount of current, and therefore power, to the output of a cell, even after accounting for typical bifaciality factors of 0.74 to 0.95 [43–45]. Provided that the relative geometry between the high albedo surface and the backside of the cells is identical, the backside illumination enhancements shown here (with individual cells) should apply to modules.

The measured current gains illustrate the potential of using nanoPAN covers to enhance the ground albedo and increase the efficiency of fielded bifacial PVs. Simulations indicate that increasing the albedo by 0.5, consistent with this work, is expected to improve the power output by 18 % under standard conditions [6] and the electricity production (annual energy yield) by 30-40% (global average) [4].

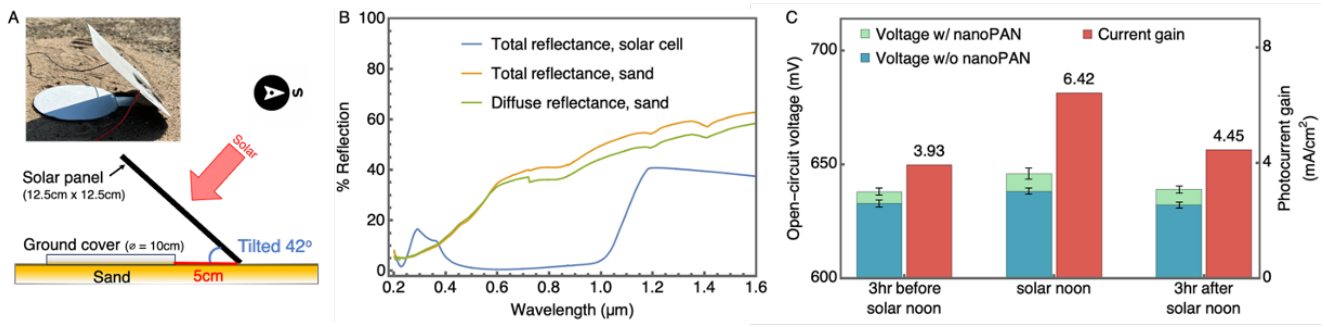

Fig. 4: (A) Schematics and images of the outdoor backside illumination test. (B) Optical property characterization of the cells and the sand used in the experiments. (C) The nanoPAN groundcover boosts the open-circuit voltage of the cells. Corresponding current gains, attributed to the improved light harvesting, are estimated using a cell model.

4 Conclusion

We have experimentally investigated a high albedo daytime radiative cooling material that is capable of enhancing the amount of light collected by a bifacial solar cell. An electrospun layer of beaded nanofibers (nanoPAN) optimizes solar-specific scattering, resulting in a $\sim 20\,\mathrm{W/m^2}$ gain in daytime radiative cooling power compared a PDMS-coated silver mirror. Additionally, the nanoPAN-based cover increases the ground albedo compared to sand, resulting in $6.42\,\mathrm{mA/cm^2}$ of additional photocurrent generated by a commercial silicon solar cell. Expected energy-yield gains exceed 18% according to simulations in literature. Future work involves investigating how the nanophotonic groundcover affects the power output and temperature of fielded biafical solar panels at the appropriate scale to capture the effects of higher albedo and lower ground-surface temperatures on the microclimate at the PV site.

5 Author Contributions

Materials fabrication: HK, EM, AH, SC. Outdoor cooling tests: HK, AH, SM, SC. Outdoor PV tests: YG, EM, AH, SC. Research design: HK, YG, AL. Writing: all authors.

6 Competing Interests

A patent has been granted related to the contents of this manuscript.

7 Acknowledgement

This material is based on work supported by the National Science Foundation under grant number 2144662 and by Michigan Economic Development Corporation under the Advance Grant. The authors also acknowledge the support of the 3M foundation and thank Bosun Roy Layinde and Andres Miranda Manon for help with materials characterization.

8 Data Availability

All study data are included in the article or available upon reasonable request.

References

[1] O. Duprénbsp;, R. Vaillon, and M. A. Green, *Thermal behavior of photovoltaic devices: Physics and engineering*. SPRINGER, 2018, vol. 10.

[2] N. M. Haegel, P. Verlinden, M. Victoria, P. Altermatt, H. Atwater, T. Barnes, C. Breyer, C. Case, S. De Wolf, C. Deline *et al.*, "Photovoltaics at multi-terawatt scale: waiting is not an option," *Science*, vol. 380, no. 6640, pp. 39–42, 2023.

[3] N. Gomez-Casanovas, P. Mwebaze, M. Khanna, B. Branham, A. Time, E. H. DeLucia, C. J. Bernacchi, A. K. Knapp, M. J. Hoque, X. Du *et al.*, "Knowns, uncertainties, and challenges in agrivoltaics to sustainably intensify energy and food production," *Cell Reports Physical Science*, 2023.

[4] U. A. Yusufoglu, T. H. Lee, T. M. Pletzer, A. Halm, L. J. Koduvelikulathu, C. Comparotto, R. Kopecek, and H. Kurz, "Simulation of energy production by bifacial modules with revision of ground reflection," *Energy Procedia*, vol. 55, pp. 389–395, 2014.

[5] X. Sun, M. R. Khan, C. Deline, and M. A. Alam, "Optimiza-

tion and performance of bifacial solar modules: A global perspective," *Applied energy*, vol. 212, pp. 1601–1610, 2018.

[6] G. Raina and S. Sinha, "A simulation study to evaluate and compare monofacial vs bifacial perc pv cells and the effect of albedo on bifacial performance," *Materials Today: Proceedings*, vol. 46, pp. 5242–5247, 2021.

[7] M. R. Khan, E. Sakr, X. Sun, P. Bermel, and M. A. Alam, "Ground sculpting to enhance energy yield of vertical bifacial solar farms," *Applied Energy*, vol. 241, pp. 592–598, 2019.

[8] X. Li, B. Sun, C. Sui, A. Nandi, H. Fang, Y. Peng, G. Tan, and P.-C. Hsu, "Integration of daytime radiative cooling and solar heating for year-round energy saving in buildings," *Nature communications*, vol. 11, no. 1, p. 6101, 2020.

[9] J. Xu, J. Zhang, B. Fu, C. Song, W. Shang, P. Tao, and T. Deng, "All-day freshwater harvesting through combined solar-driven interfacial desalination and passive radiative cooling," *ACS Applied Materials & Interfaces*, vol. 12, no. 42, pp. 47 612–47 622, 2020.

[10] I. Haechler, H. Park, G. Schnoering, T. Gulich, M. Rohner, A. Tripathy, A. Milionis, T. M. Schutzius, and D. Poulikakos, "Exploiting radiative cooling for uninterrupted 24-hour water harvesting from the atmosphere," *Science Advances*, vol. 7, no. 26, p. eabf3978, 2021.

[11] X. Zhang, W. Yang, Z. Shao, Y. Li, Y. Su, Q. Zhang, C. Hou, and H. Wang, "A moisture-wicking passive radiative cooling hierarchical metafabric," *ACS nano*, vol. 16, no. 2, pp. 2188–2197, 2022.

[12] Z. Xia, Z. Fang, Z. Zhang, K. Shi, and Z. Meng, "Easy way to achieve self-adaptive cooling of passive radiative materials," *ACS applied materials & interfaces*, vol. 12, no. 24, pp. 27 241–27 248, 2020.

[13] G. B. Smith and C. G. Granqvist, *Coolness: High-Albedo Surfaces and Sky Cooling*. CRC Press, Taylor, Francis Group, 2011, p. 58.

[14] C. A. Bankston, *Solar heat technologies: fundamentals and applications*. Cambridge, Massachusetts: MIT Press, 1900.

[15] D. Zhao, A. Aili, Y. Zhai, S. Xu, G. Tan, X. Yin, and R. Yang, "Radiative sky cooling: Fundamental principles, materials, and applications," *Applied Physics Reviews*, vol. 6, no. 2, p. 021306, 2019.

[16] M. M. Hossain and M. Gu, "Radiative cooling: principles, progress, and potentials," *Advanced Science*, vol. 3, no. 7, p. 1500360, 2016.

[17] A. P. Raman, M. A. Anoma, L. Zhu, E. Rephaeli, and S. Fan, "Passive radiative cooling below ambient air temperature under direct sunlight," *Nature*, vol. 515, no. 7528, pp. 540–544, 2014.

[18] Z. Chen, L. Zhu, A. Raman, and S. Fan, "Radiative cooling to deep sub-freezing temperatures through a 24-h day–night cycle," *Nature communications*, vol. 7, no. 1, p. 13729, 2016.

[19] D. Wu, C. Liu, Z. Xu, Y. Liu, Z. Yu, L. Yu, L. Chen, R. Li, R. Ma, and H. Ye, "The design of ultra-broadband selective near-perfect absorber based on photonic structures to achieve near-ideal daytime radiative cooling," *Materials & Design*, vol. 139, pp. 104–111, 2018.

[20] J.-l. Kou, Z. Jurado, Z. Chen, S. Fan, and A. J. Minnich, "Daytime radiative cooling using near-black infrared emitters," *Acs Photonics*, vol. 4, no. 3, pp. 626–630, 2017.

[21] Y. Zhai, Y. Ma, S. N. David, D. Zhao, R. Lou, G. Tan, R. Yang, and X. Yin, "Scalable-manufactured randomized glass-polymer hybrid metamaterial for daytime radiative cooling," *Science*, vol. 355, no. 6329, pp. 1062–1066, 2017.

[22] S. Atiganyanun, J. B. Plumley, S. J. Han, K. Hsu, J. Cytrynbaum, T. L. Peng, S. M. Han, and S. E. Han, "Effective radiative cooling by paint-format microsphere-based photonic random media," *ACS Photonics*, vol. 5, no. 4, pp. 1181–1187, 2018.

[23] X. Wang, X. Liu, Z. Li, H. Zhang, Z. Yang, H. Zhou, and T. Fan, "Scalable flexible hybrid membranes with photonic structures for daytime radiative cooling," *Advanced Functional Materials*, vol. 30, no. 5, p. 1907562, 2020.

[24] J. Yang, X. Gao, Y. Wu, T. Zhang, H. Zeng, and X. Li, "Nanoporous silica microspheres–ploymethylpentene (tpx) hybrid films toward effective daytime radiative cooling," *Solar Energy Materials and Solar Cells*, vol. 206, p. 110301, 2020.

[25] H. Bao, C. Yan, B. Wang, X. Fang, C. Zhao, and X. Ruan, "Double-layer nanoparticle-based coatings for efficient terrestrial radiative cooling," *Solar Energy Materials and Solar Cells*, vol. 168, pp. 78–84, 2017.

[26] X. Li, J. Peoples, Z. Huang, Z. Zhao, J. Qiu, and X. Ruan, "Full daytime sub-ambient radiative cooling in commercial-like paints with high figure of merit," *Cell Reports Physical Science*, vol. 1, no. 10, p. 100221, 2020.

[27] J. D. Alden, S. Atiganyanun, R. Vanderburg, S. H. Lee, J. B. Plumley, O. K. Abudayyeh, S. M. Han, and S. E. Han, "Radiative cooling by silicone-based coating with randomly distributed microbubble inclusions," *Journal of Photonics for Energy*, vol. 9, no. 3, pp. 032 705–032 705, 2019.

[28] J. Zhang, Z. Zhou, H. Tang, J. Xing, J. Quan, J. Liu, J. Yu, and M. Hu, "Mechanically robust and spectrally selective convection shield for daytime subambient radiative cooling," *ACS Applied Materials & Interfaces*, vol. 13, no. 12, pp. 14 132–14 140, 2021.

[29] D. Li, X. Liu, W. Li, Z. Lin, B. Zhu, Z. Li, J. Li, B. Li, S. Fan, J. Xie *et al.*, "Scalable and hierarchically designed polymer film as a selective thermal emitter for high-performance all-day radiative cooling," *Nature Nanotechnology*, vol. 16, no. 2, pp. 153–158, 2021.

[30] H. Kim, S. McSherry, B. Brown, and A. Lenert, "Selectively enhancing solar scattering for direct radiative cooling through control of polymer nanofiber morphology," *ACS Applied Materials & Interfaces*, vol. 12, no. 39, pp. 43 553–43 559, 2020.

[31] E. Torgerson and J. Hellhake, "Polymer solar filter for enabling direct daytime radiative cooling," *Solar Energy Materials and Solar Cells*, vol. 206, p. 110319, 2020.

[32] A. Leroy, B. Bhatia, C. C. Kelsall, A. Castillejo-Cuberos, M. Di Capua H, L. Zhao, L. Zhang, A. Guzman, and E. Wang, "High-performance subambient radiative cooling enabled by optically selective and thermally insulating polyethylene aerogel," *Science advances*, vol. 5, no. 10, p. eaat9480, 2019.

[33] J. Mandal, Y. Fu, A. C. Overvig, M. Jia, K. Sun, N. N. Shi, H. Zhou, X. Xiao, N. Yu, and Y. Yang, "Hierarchically porous polymer coatings for highly efficient passive daytime radiative cooling," *Science*, vol. 362, no. 6412, pp. 315–319, 2018.

[34] H. Kim and A. Lenert, "Optical and thermal filtering

nanoporous materials for sub-ambient radiative cooling," *Journal of Optics*, vol. 20, no. 8, p. 084002, 2018.

[35] J. Chen and L. Lu, "Development of radiative cooling and its integration with buildings: A comprehensive review," *Solar Energy*, vol. 212, pp. 125–151, 2020.

[36] X. Li, J. Peoples, P. Yao, and X. Ruan, "Ultrawhite baso4 paints and films for remarkable daytime subambient radiative cooling," *ACS Applied Materials & Interfaces*, vol. 13, no. 18, pp. 21 733–21 739, 2021.

[37] S. Sreenath, K. Sudhakar, and A. Yusop, "Solar pv in the airport environment: A review of glare assessment approaches & metrics," *Solar Energy*, vol. 216, pp. 439–451, 2021.

[38] R. Chiabrando, E. Fabrizio, and G. Garnero, "The territorial and landscape impacts of photovoltaic systems: Definition of impacts and assessment of the glare risk," *Renewable and Sustainable Energy Reviews*, vol. 13, no. 9, pp. 2441–2451, 2009.

[39] T. Rose and A. Wollert, "The dark side of photovoltaic—3d simulation of glare assessing risk and discomfort," *Environmental Impact Assessment Review*, vol. 52, pp. 24–30, 2015.

[40] B. Roy-Layinde, T. Burger, D. Fan, B. Lee, S. McSherry, S. R. Forrest, and A. Lenert, "Sustaining efficiency at elevated power densities in ingaas airbridge thermophotovoltaic cells," *Solar Energy Materials and Solar Cells*, vol. 236, p. 111523, 2022.

[41] A. Berk, G. P. Anderson, P. K. Acharya, L. S. Bernstein, L. Muratov, J. Lee, M. Fox, S. M. Adler-Golden, J. H. Chetwynd Jr, M. L. Hoke *et al.*, "Modtran5: 2006 update," in *Algorithms and technologies for multispectral, hyperspectral, and ultraspectral imagery xii*, vol. 6233. Bellingham, WA: SPIE, 2006, pp. 508–515.

[42] B. Ross and J. E. Walsh, "A comparison of simulated and observed fluctuations in summertime arctic surface albedo," *Journal of Geophysical Research: Oceans*, vol. 92, no. C12, pp. 13 115–13 125, 1987.

[43] R. Kopecek and J. Libal, "Bifacial photovoltaics 2021: Status, opportunities and challenges," *Energies*, vol. 14, no. 8, p. 2076, 2021.

[44] Q. Bai, H. Tian, C. Nan, L. Ouyang, Y. Zhang, J. Ma, S. Mao, H. Han, H. Yang, and H. Wang, "Investigation on bifaciality factor and ideality factor of perc bifacial solar module under different irradiances," in *2021 IEEE 48th Photovoltaic Specialists Conference (PVSC)*. Piscataway, NJ: IEEE, 2021, pp. 0248–0251.

[45] D. Chen, S. Pang, L. Zhou, X. Li, A. Su, W. Zhu, J. Chang, J. Zhang, C. Zhang, and Y. Hao, "An efficient teo 2/ag transparent top electrode for 20%-efficiency bifacial perovskite solar cells with a bifaciality factor exceeding 80%," *Journal of Materials Chemistry A*, vol. 7, no. 25, pp. 15 156–15 163, 2019.